

Choice of Discrete Element Simulation Contact Model Parameter to Reproduce Laboratory Surface Avalanche

Fu-Ling Yang¹, Chuin-Shan Chen^{2*}, Wei-Tze Chang³, Shang-Hsien Hsieh²

1 Department of Mechanical Engineering, National Taiwan University, Taipei, TAIWAN

2 Department of Civil Engineering, National Taiwan University, Taipei, TAIWAN

3 National Center for Research on Earthquake Engineering, Taipei, TAIWAN

1)fulingyang@ntu.edu.tw

ABSTRACT

This work presents a method to assign soft-sphere contact parameters in a discrete- element (DE) simulation with which we can reproduce the experimentally measured avalanche dynamics of finite dry spheres down a flume at different inclination angles. We adopt the simplest linear model and the model spring and damping constants are chosen uniquely to satisfy elasticity models or to meet experimental evidences at the particle size level, namely the Hertzian contact time and the measured coefficient of restitution. We follow the literature to assign the tangential spring constant according to elasticity model but propose a method to assign the friction coefficient using a measured bulk property that characterizes the bulk discharge volume flow rate. The developed contact model was evaluated by comparing the simulated bulk avalanche dynamics down three slopes to the experimental data: including instantaneous particle trajectories and bulk unsteady velocity profile. Satisfying quantitative agreement was obtained except at the free surface and the early-time front propagation velocity.

1. INTRODUCTION

Discrete element (DE) simulation has been a popular means to study the dynamics and the rheological behavior of granular flows since the constituent is discrete in nature (Cundal & Strack 1979; GDR Midi 2004; da Cruz *et. al* 2004; Campbell 2006). Individual particle interactions are described by various contact models of different complexity and require the user to specify model parameters to characterize the material elastic and dissipating properties (Mindlin & Deresiewicz 1953; Cundall & Strack 1979; Walton & Braun 1986; Walton 1993). In general, qualitatively similar flow phenomenon can be generated as long as the contact parameters are not set to extreme values (often zero is problematic) and numerical simulation has been successful on extrapolating flow physics (GDR Midi 2004, da Cruz *et. al* 2005).

Nonetheless, when it comes to industrial design or prevention of nature hazards, quantitative prediction is crucial and remains uncertain and challenging as noted by many researchers. The existing works that attempt for quantitative predictions rely on certain calibration procedures that vary greatly from cases to cases according to contact models and flow geometries (Valention *et. al* 2008; Banton *et. al* 2009; Rycroft *et. al* 2009; Teufelsbauer *et. al* 2009, 2012). Hence, this work proposes a simple and easy-to-calibrate method to assign contact model parameters for DE simulation of unsteady surface granular flows.

2. PROBLEM SETUP: EXPERIMENT AND SIMULATION

We consider the avalanche of finite monotonic dry spheres down a flume tilted at $\theta=19^\circ$, 24° , and 29° as sketched in Fig.1. The reservoir is made of glass sidewalls and smooth aluminum base in the dimension of 35cm in length, 15cm in width (W), and 45cm in height. A gate was installed with a pair of strong compression springs to hold the granular material and a granular avalanche was initiated by releasing the gate abruptly. We used nearly identical glass spheres of diameter $D = 1.6\text{cm}$ and density $2.54 \pm 0.04\text{g/cm}^3$. A total weight of 16kg was poured into the reservoir in an arbitrary manner and the free surface was leveled manually before each experiment.

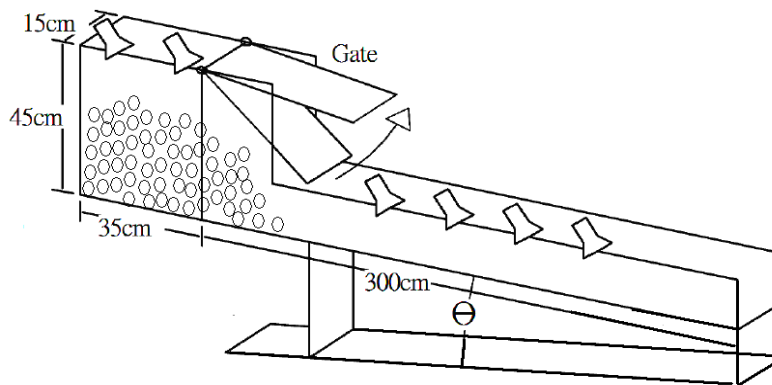


Fig. 1 Schematic diagram of the flume facility

In the simulation, the geometry and properties of the sphere and the flume are set identical to that adopted in the experiments. The sphere motion was recorded with a lateral high-speed digital camera in the experiments which gives only the images at the flume lateral side-wall since the adopted glass spheres are opaque. Hence, we only examined the simulated spheres adjacent to the wall when we calibrated the numerical results with the experimental data. We have developed an image processing routine to

track individual sphere velocity by the method of particle tracking velocimetry (PTV) using a specific elapsed time $\Delta T = 2 \times 10^{-3}$ s. Note that this elapsed time is much greater than the time step, $dt = 10^{-6}$ s, in DE simulation. Hence, we used the simulated particle positions at two times ΔT apart to estimate a displacement and divided it by ΔT to obtain particle velocity vector, which is consistent to the experimental PTV procedure.

The sphere motions obtained from experiments or simulations were averaged alike by an area-weighted scheme to calculate a continuum-like bulk velocity as

$$\vec{U}(t, x, y) = \frac{\sum_i A_i(t) \vec{u}_i(t)}{\sum_i A_i(t)}.$$

Here, \vec{u}_i and A_i are the instantaneous sphere velocity and its projected area that overlaps with an averaging box located at (x, y) in a rectangular coordinate system defined at the reservoir rear base corner. The formula is derived from the total momentum conservation and we chose the averaging box to be a square of 2D side-length, with D being the sphere diameter. By shifting the averaging box along y by D , we can obtain an instantaneous velocity depth profile at specific t and x .

3. CONTACT MODEL AND PARAMETER ASSIGNMENT

A parallel DE simulation code has been developed and used for this simulation. Each sphere motion is updated according to its interaction force with neighboring spheres calculated by a linear soft-sphere contact model whose schematic diagram is shown in Fig. 2(b). When two spheres come into contact at different velocities, surface deformation occurs at the contact point resulting in displacements of the sphere centers along and perpendicular to the contact normal, \vec{n} , defined by the line of centers. Their relative velocity is decomposed correspondingly into a normal and a tangential component, u_n and u_t . Along \vec{n} , two normal forces arise due to normal elastic and plastic deformation: one restoring spring force, $F_{n1} = k_n d_n$, and one dissipating force, $F_{n2} = c_n u_n$. Here, k_n and c_n are the normal spring and damping constants and d_n is the total normal displacement during a contact tracked in an incremental form with a constant time step $dt = 10^{-6}$ s. Meanwhile, lateral deformation grows to generate a tangential restoring spring force, $F_{t1} = k_t d_t$ with incremental d_t . When the tangential deformation reaches a yielding condition, sliding contact occurs and the resulting frictional force is modeled by Coulomb's law as $F_{t2} = f(F_{n1} + F_{n2})$. The tangential interaction force is assigned to F_{t2} when $|F_{t2}| > |F_{t1}|$ and F_{t1} is applied otherwise, allowing sliding-sticking switch during a contact.

To assign k_n , c_n , and k_t for a paired interaction, the governing equation of d_n

namely $m^*\ddot{d}_n + c_n\dot{d}_n + k_nd_n = 0$, is solved with initial conditions $d_n(0) = 0$ and $\dot{d}_n(0) = u_n$. Here, $m^* = m/2$ is the effective mass. The instant for $d_n = 0$ determines the contact duration as $\tau = \pi\sqrt{k_n(1 - c_n^2)/m^*}$ and the rebound relative velocity is $\dot{d}_n(\tau)$. A coefficient of restitution can then be calculated for a simulated contact as $e = \exp[\sqrt{-\pi c_n/(1 - c_n^2)}]$. Thus, an assigned e determines a c_n that is further employed to give k_n to reproduce the Hertzian contact time by requiring $\tau = \tau_{Hertz} = 2.87/a^*(m^*/E^*)^{2/5}|U_n|^{-1/5}$ from the simulation. Here, $E^* = E/[2(1 - \nu)]$ is the effective Young's modulus with ν and E denoting the Poisson's ratio and Young's modulus of spheres. For the tangential contact parameter, we assign $k_t = 2/(2 - \nu^*) [3G^{*2}(1 - \nu^*)|F_{n1} + F_{n1}|]^{1/3}$ with $\nu^* = \nu/2$ and $G^* = G/2$ is the effective shear modulus (Cundall & Strack 1979). The only free parameter left unspecified is the tangential friction coefficient f . Though the tribology literature provides extensive information about the friction coefficients for the present surface combinations, the values could vary by one order of magnitude. In addition, these factors are usually measured in quasi-steady loading condition, which is rarely met during an unsteady contact in an evolving bulk. Considering that the ultimate goal of our DE simulation is to capture bulk dynamics, we decided to choose a feasible f by reproducing the bulk volume discharge rate $Q(t)$ measured in the experiment. Under the assumption of nearly two-dimensional flow in this narrow flume of width W , $Q(t)$ can be equivalently presented by the bulk remaining volume in the reservoir, $V(t) = A(t)W$ with $A(t)$ denoting the bulk projection area on the reservoir wall. Note that the time rate of change of $A(t)$ gives the desired $Q(t)$.

Hence, a set of trial simulations were conducted using various f s for sphere-sphere, sphere-base, and sphere-wall tangential interactions which values are denoted by (f^{ss}, f^{sb}, f^{sw}) . For each combination, the simulated sphere locations were projected onto the reservoir wall to obtain $A(t)$ which is compared to the experimental data after normalization with their initial values in Fig.2. The set (f^{ss}, f^{sb}, f^{sw}) that gives the least deviation from the measured $A(t)$ is determined as the most feasible friction coefficient and hence we continue to evaluate if the corresponding simulation results feasibly reproduce the experimental data.

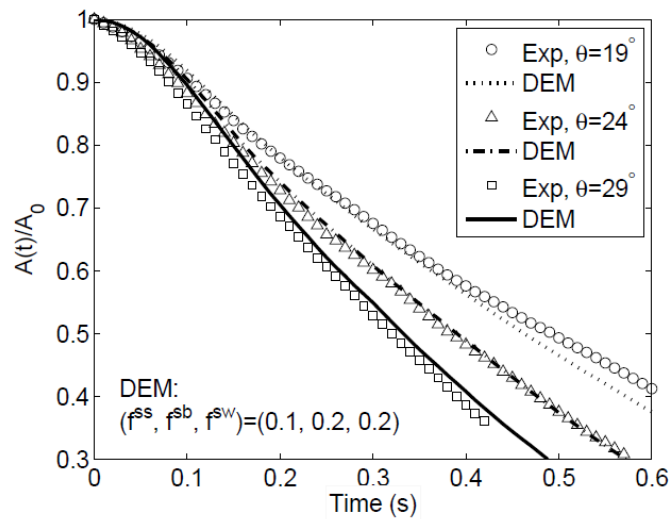


Fig.2 Comparison of the simulated temporal profile of the normalized projection area to those measured in the experiments at three reservoir inclination angles.

4. COMPARISON OF SIMULATED AND EXPERIMENTAL BULK DYNAMICS

4.1 Trajectory of individual spheres

The best-fitted simulation was firstly evaluated *at the particle size level* by comparing the individual sphere trajectory adjacent to the flume sidewall to that measured in the experiments when the flume was at $\theta=19^\circ$. To achieve this, three groups of tracer spheres were selected from the experimental images at different streamwise positions (rear, central, and front group). The numerically created spheres were then examined to identify those with the shortest distance to each experimental tracer sphere. The simulated trajectories for $t=0\sim 0.45s$ are shown by the solid lines which follow those measured in the experiments as portrayed by open circles in Fig.3.

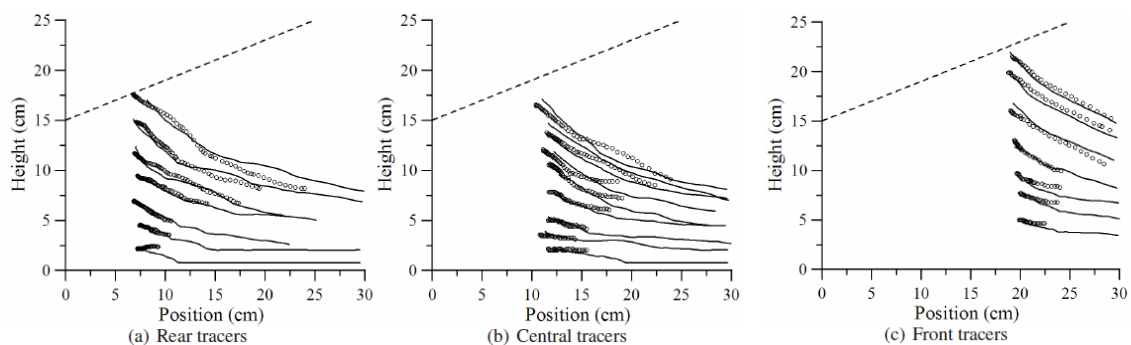


Fig.3 Comparison of the simulated and the measured trajectories of individual spheres moving next to the reservoir wall in a dry granular avalanche at $\theta=19^\circ$.

4.2 Bulk streamwise velocity

The individual sphere motions were then averaged as described above to obtain instantaneous depth profile for bulk streamwise velocity. Fig. 4 compares the results for the avalanche at $\theta=19^\circ$ at $t = 0.1, 0.2,$ and 0.3 second after gate opening. Three probing locations were adopted at $x = 8, 16,$ and 24 cm and one simulation result is compared to the mean of three repeated experiments. General agreement between the numerical and experimental results is clearly seen except near the free surface at $t = 0.1$ second and the front motion at $t = 0.3$ second. The free surface deviation is speculated to result from differences in the initial packing which can cause local particle rearrangement and hence affected the instantaneous local velocity. Similar agreement between the numerical and experimental results can also be obtained for $\theta=24^\circ$ and 29° and in Fig.5 we show the comparison of repeated simulations with the mean measured value for $\theta=29^\circ$.

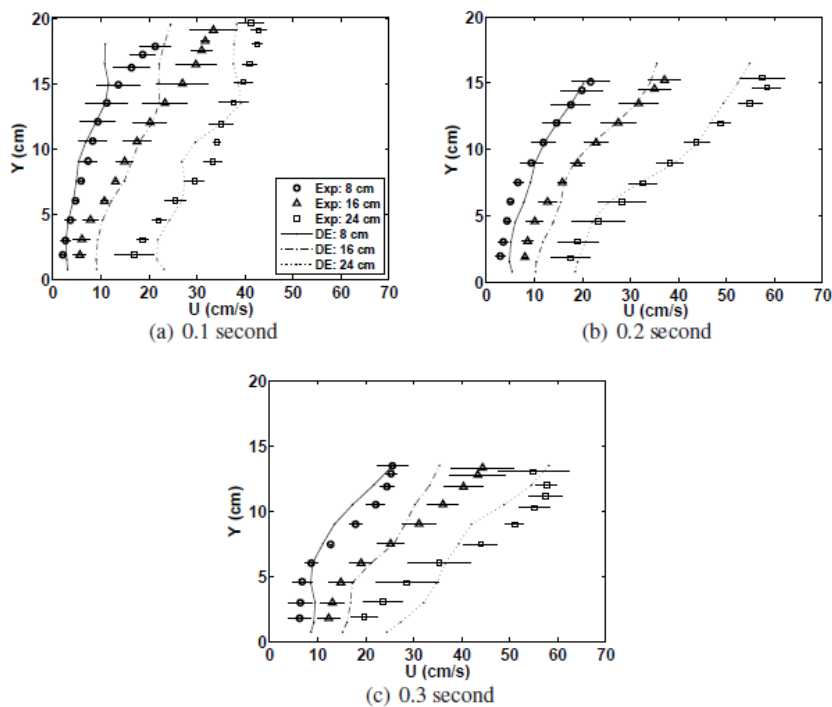


Fig.4 Comparison of the simulated and the measured instantaneous bulk velocity profile at $x=8, 16,$ and 24 cm at $t=(a) 0.1$ s, $(b) 0.2$ s, and $(c) 0.3$ s after the gate opening ($\theta=19^\circ$).

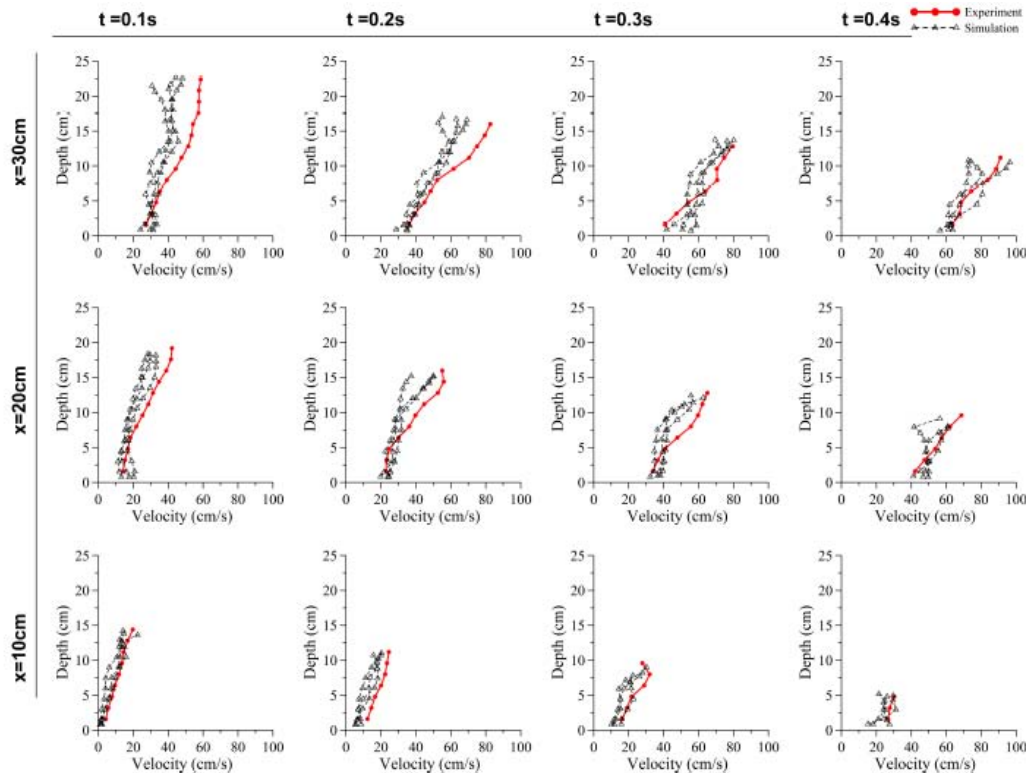


Fig.5 Comparison of the instantaneous bulk velocity from three simulations to the mean of three experiments at different times and positions ($\theta=29^\circ$).

5. CONCLUSION

A discrete-element simulation scheme that utilizes a linear soft-sphere contact model has been developed to simulate the avalanche process of finite dry spheres down a reservoir at three inclination angles, 19° , 24° , and 29° . We propose a method to assign the contact model parameters by theoretical models for paired contacting surfaces or existing experimental evidences. We then compared the simulated bulk motion, with the selected f_s , to that measured in the experiments. Satisfying agreement was obtained on the trajectory of individual spheres and the instantaneous bulk velocity depth profiles half-way through the unsteady process. It is thus concluded that the current method for selecting feasible friction coefficients and the rest contact model parameters is effective to reproduce the general feature of actual dry granular avalanche processes with DE simulations.

REFERENCES

P.A. Cundall and O.D. L. Strack (1979) "A discrete numerical model for granular

- assemblies," *Geotechnique* 29(1), 47-65
- GDR MiDi (2004) "On dense granular flows," *Eur. Phys. J. E* 14, 341-365
- F. da Cruz, S. Emam, M. Prochnow, J.-N. Roux and F. Chevoir (2005) "Rheophysics of dense granular materials: discrete simulation of plane shear flows," *Phys. Rev. E* 72, 021309
- C. S. Campbell (2006) "Granular material flows: an overview," *Powder Technology* 162, 208-229
- R. D. Mindlin and H. Deresiewicz (1953) "Elastic spheres in contact under varying oblique forces," *J. Applied Mech.* 20, 327
- O.R. Walton and R.L. Braun (1986) "Viscosity, granular-temperature, and stress calculations for shearing assemblies of inelastic, frictional disks," *J. Rheol.* 30(5), 949-980
- O.R. Walton (1993) "Numerical simulation of inclined chute flows of monodisperse, inelastic, frictional spheres," *Mechanics of Materials* 16, 239-247
- R. Valention, G. Baria and L. Montrasio, (2008) "Experimental analysis and micromechanical modeling of dry granular flow and impacts in laboratory flume tests," *Rock Mech. Rock Engng*, 41(1), 153-177
- J. Banton, P. Villard, D. Jongmans and C. Scavia (2009) "Two-dimensional discrete element models of debris avalanches: Parameterization and the reproducibility of experimental results," *J. Geophysical Research*, 114 , F04013
- C. H. Rycroft, A. V. Orpe, A. Kudrolli (2009) "Physical test of a particle simulation model in a sheared granular system," *Phys. Rev. E*, 80, 031305
- H. Teufelsbauer, Y. Wang, M.-C. Chiou and W. Wu (2009) "Flow-obstacle interaction in rapid granular avalanches, DEM simulation and comparison with experiment," *Granular Matter*, 11, 209-220
- H. Teufelsbauer, Y. Wang, S.P. Pudasaini, R.I. Borja, and W. Wu (2012) "DEM simulation of impact force exerted by granular flow on rigid structures," *Acta Geotechnica*, 6(3), 119-133